15. Neumeyer JL, Wang S, Gao Y, et al. *N*-ω-Fluoroalkyl analogs of (1R)−2β-carbomethoxy-3-β-(4-iodophenyl)-tropane (β-CIT): radiotracers for positron emission tomography and single photon emission CT imaging of dopamine transporters. *J Med Chem* 1994;37:1558–1561.
16. Baldwin RM, Zea-Ponce Y, Al-Tikriti MS, et al. Regional brain uptake and pharmacokinetics of [^{123}I]*N*-ω-fluoroalkyl-2β-carboxy-3β-(4-iodophenyl)nortropane esters in baboons. *Nucl Med Biol* 1995;22:211–219.
17. Neumeyer JL, Tamagnan G, Wang S, et al. *N*-substituted analogs of 2β-carbomethoxy-3β-(4′-iodophenyl)tropane (β-CIT) with selective affinity to dopamine or serotonin transporters in rat forebrain. *J Med Chem* 1996;39:543–548.
18. Lundkvist C, Halldin C, Swahn C-G, et al. [*O*-methyl-^{11}C]β-CIT-FP, a potential radioligand for quantitation of the dopamine transporter: preparation, autoradiography, metabolic studies, and positron emission tomography examinations. *Nucl Med Biol* 1995;22:905–913.
19. Chaly T, Dhawan V, Kazumata K, et al. Radiosynthesis of [^{18}F]*N*−3-fluoropropyl-2-β-carbomethoxy-3-β-(4-iodophenyl)nortropane and the first human study with positron emission tomography. *Nucl Med Biol* 1996;23:999–1004.
20. Kuikka JT, Bergström KA, Ahonen A, et al. Comparison of iodine-123 labelled 2β-carbomethoxy-3β-(4-iodophenyl)tropane and 2β-carbomethoxy-3β-(4-iodophenyl)-*N*-(3-fluoropropyl)nortropane for imaging of the dopamine transporter in the living human brain. *Eur J Nucl Med* 1995;22:356–360.
21. Abi-Dargham A, Gandelman MS, DeErausquin GA, et al. SPECT imaging of dopamine transporters in human brain with iodine-123-fluoroalkyl analogs of β-CIT. *J Nucl Med* 1996;37:1129–1133.
22. Booij J, Tissingh G, Winogrodzka A, et al. Practical benefit of [^{123}I]FP-CIT SPET in the demonstration of the dopaminergic deficit in Parkinson's disease. *Eur J Nucl Med* 1997;24:68–71.
23. Booij J, Tissingh G, Boer GJ, et al. [^{123}I]FP-CIT SPECT shows a pronounced decline of striatal dopamine transporter labelling in early and advanced Parkinson's disease. *J Neurol Neurosurg Psychiatry* 1997;62:133–140.
24. Hughes AJ, Daniel SE, Kilford L, Lees AJ. Accuracy of clinical diagnosis of idiopathic Parkinson's disease: a clinico-pathological study of 100 cases. *J Neurol Neurosurg Psychiatry* 1992;55:181–184.
25. Fahn S, Elton R. Members of the UPDRS development committee. Unified Parkinson's disease rating scale. In: Fahn S, Marsden CD, Calne DB, Goldstein M, eds. *Recent developments in Parkinson's disease*. Florham Park, NJ: Macmillan Healthcare Information; 1987:153–164.
26. Hoehn MM, Yahr MD. Parkinsonism: onset, progression, and mortality. *Neurology* 1967;17:427–442.
27. Hughes A, Lees AJ, Stern GM. Apomorphine test to predict dopaminergic responsiveness in Parkinsonian syndromes. *Lancet* 1990;336:32–34.
28. Ikawa K, Watanabe A, Kaneno S, Toru M. Modulation of [^{3}H]mazindol binding sites in rat striatum by dopaminergic agents. *Eur J Pharmacol* 1993;250:261–266.
29. Laruelle M, Baldwin RM, Malison RT, et al. SPECT imaging of dopamine and serotonin transporters with [^{123}I]β-CIT: pharmacological characterization of brain uptake in nonhuman primates. *Synapse* 1993;13:295–309.
30. Ishikawa T, Dhawan V, Kazumata K, et al. Comparative nigrostriatal dopaminergic imaging with iodine-123-βCIT-FP/SPECT and fluorine-18-FDOPA/PET. *J Nucl Med* 1996;37:1760–1765.
31. Kish SJ, Shannak K, Hornykiewicz O. Uneven pattern of dopamine loss in the striatum of patients with idiopathic Parkinson's disease. *N Engl J Med* 1988;876:876–880.
32. Goto S, Hirano A, Matsumoto S. Subdivisional involvement of nigrostriatal loop in idiopathic Parkinson's disease and striatonigral degeneration. *Ann Neurol* 1989;26:766–770.
33. Gibb WRG, Lees AJ. Anatomy, pigmentation, ventral and dorsal subpopulations of the substantia nigra, and differential cell death in Parkinson's disease. *J Neurol Neurosurg Psychiatry* 1991;54:388–396.
34. Van Dyck CH, Seibyl JP, Malison RT, et al. Age-related decline in striatal dopamine transporter binding with iodine-123-β-CIT SPECT. *J Nucl Med* 1995;36:1175–1181.
35. Volkow ND, Ding Y-S, Fowler JS, et al. Dopamine transporters decrease with age. *J Nucl Med* 1996;37:554–559.
36. Tissingh G, Bergmans P, Booij J, et al. Nigrostriatal dopaminergic imaging with iodine-123-βCIT-FP/SPECT and fluorine-18-FDOPA/PET [Letter]. *J Nucl Med* 1997;37:1271–1272.
37. Tissingh G, Bergmans P, Booij J, et al. Drug-naive patients with Parkinson's disease in Hoehn & Yahr stage I and II show a bilateral decrease in striatal dopamine transporters as revealed by [^{123}I]β-CIT SPECT. *J Neurol* 1998;245:14–20.
38. Seibyl J, Marek K, Sheff K, Neumeyer J, Innis R. Comparison of [I-123]FP-CIT and [I-123]β-CIT for SPECT imaging of dopamine transporters in Parkinson's disease [Abstract]. *J Nucl Med* 1996;37(suppl):133.

5-[^{125}I]Iodo-2′-Deoxyuridine in the Radiotherapy of Brain Tumors in Rats

Amin I. Kassis, Patrick Y. Wen, Annick D. Van den Abbeele, Janina Baranowska-Kortylewicz, G. Mike Makrigiorgos, Kenneth R. Metz, Khalid Z. Matalka, Colin U. Cook, Shailendra K. Sahu, Peter McL. Black and S. James Adelstein
Departments of Radiology, Neurology and Neurosurgery, Harvard Medical School, Boston, Massachusetts

Glial neoplasms of the human central nervous system have defied treatment, in part because of the limited selectivity of available cytotoxic agents. The thymidine analog 5-iodo-2′-deoxyuridine radiolabeled with the Auger electron emitter ^{125}I (^{125}IUdR) is highly toxic to dividing cells when it is deoxyribonucleic acid incorporated, but it is relatively innocuous when located outside the nucleus. Previous studies have shown that ^{125}IUdR has significant antineoplastic potential against mammalian cells in vitro and direct administration of ^{125}IUdR is effective therapy for ovarian ascites tumors in mice and neoplastic meningitis in rats. Studies using external gamma imaging and autoradiography have also shown that direct intratumoral administration of ^{123}IUdR/^{125}IUdR into intracerebral 9L gliosarcomas in rats results in selective uptake of the radionuclide into tumor cells. Based on these encouraging results, we have evaluated the therapeutic potential of ^{125}IUdR in rats bearing intracerebral 9L gliosarcomas. **Methods:** Iodine-125-IUdR was infused intracerebrally over a 2-day period into rats bearing 1-day-old 9L tumors and over a 6-day period into animals with 9-day-old 9L tumors; equimolar concentrations of ^{127}IUdR were infused into control animals. Tumor growth was monitored by contrast-enhanced ^{1}H MRI and animal survival was followed over time. **Results:** Intracerebral tumors (3–7 mm) were readily detected by MRI. Tumor-bearing rats treated with ^{127}IUdR succumbed within 17–24 days, whereas tumor-bearing animals treated with ^{125}IUdR survived significantly longer, and 10%–20% of the animals were cured of tumors. **Conclusion:** These data substantiate the antineoplastic potential of 5-[^{125}I]iodo-2′-deoxyuridine and indicate that it may be a useful agent for the therapy of solid tumors that are accessible to direct radiopharmaceutical administration.

Key Words: 5-iodo-2′-deoxyuridine; Auger electrons; iodine-125; brain tumor therapy; locoregional administration

J Nucl Med 1998; 39:1148–1154

Malignant gliomas account for approximately half of the 17,500 primary brain tumors diagnosed in patients in the U.S. each year (*1,2*). Despite treatment with surgery, radiotherapy and chemotherapy, the prognosis for these patients remains poor. Median survival is 9–12 mo for patients with glioblastomas and 24–36 mo for patients with anaplastic astrocytomas (*3*). Efforts to improve the prognosis of patients with malignant gliomas have included advances in neurosurgical techniques (*4*), novel approaches to increasing the effectiveness of radiotherapy (*3,5–7*), stereotactic brachytherapy and radiosurgery (*8*), immunotherapy (*9,10*), boron-capture therapy (*11*) and, most recently, gene therapy (*12–15*). Despite these therapeutic approaches, there has been only minimal improvement in the prognosis of patients with malignant gliomas over the past two

Received Apr. 8, 1997; revision accepted Oct. 13, 1997.
For correspondence or reprints contact: Amin I. Kassis, PhD, Department of Radiology, Harvard Medical School, Goldenson Building, 220 Longwood Ave., Boston, MA 02115.

decades. The fundamental problem lies in the difficulty of total removal or effective eradication of the tumor. This impasse motivates the search for alternative treatment modalities that will show preferential uptake and selective killing of tumor cells.

Iodine-125 is a radionuclide that decays by electron capture and internal conversion. The primary vacancies in the inner electronic shells of the daughter atoms lead to the emission of a shower of low-energy (<1 keV), short-range electrons. These electrons (≈20) dissipate their energy in the immediate vicinity of the decaying atom and deposit 10^9 to 10^6 cGy per decay within 1- to 10-nm spheres (*16*). When this radionuclide in the form of the thymidine analog 5-iodo-2′-deoxyuridine (^{125}IUdR) is incorporated into deoxyribonucleic acid (DNA), it is highly cytotoxic to mammalian cells in vitro and exhibits antineoplastic activity in mice bearing an intraperitoneal murine ovarian ascites tumor and in rats with neoplastic meningitis without producing overt signs of normal tissue toxicity (*17,18*). In contrast, the decay of this radionuclide within the cell cytoplasm (*19,20*) or extracellularly (*16,20*) produces no extraordinary lethal effects. Our experience with this and several other Auger electron emitters (*21,22*) has substantiated theoretical dosimetric expectations and reiterated the dependence of Auger-electron-emitter toxicity on the intranuclear DNA localization of the radionuclide.

In previous studies, we administered a mixture of ^{123}IUdR/^{125}IUdR stereotactically into rats bearing intracerebral gliosarcomas (*23*) and obtained the following results: (a) external gamma imaging (^{123}I) visualized intracerebral tumors as small as 0.5 mm in diameter; (b) the localization of radioactivity in tumor cells, as demonstrated by autoradiography [ARG], was highly specific; (c) no DNA-incorporated radioactivity could be demonstrated in normal brain tissues (except in some endothelial cells lining the capillaries); and (d) radioactivity was visible only within the stomach and bladder outside the brain region of tumor-bearing animals. However, no DNA-incorporated activity could be demonstrated by ARG in the cells of these tissues (nor was it present in any cells of other normal tissues), suggesting that this activity most likely represented free iodide or iodinated metabolites that were not incorporated into DNA. Encouraged by these preliminary findings, we have examined the therapeutic potential of ^{125}IUdR in an intracerebral 9L gliosarcoma animal tumor model after direct intracerebral infusion. The results indicate that this radiopharmaceutical may be a useful agent for the therapy of solid tumors that are accessible to direct radiopharmaceutical administration.

MATERIALS AND METHODS

Synthesis of 5-[^{125}I]Iodo-2′-Deoxyuridine (^{125}IUdR)

2′-Deoxyuridine (0.50 g, 2.20 mmol) was dissolved in water (2 ml), the solution was heated to 50°C and mercuric acetate (0.74 g, 2.32 mmol) in 3 ml water was added. After the reaction, mixture was heated at 50°C for 2.5 hr, the vial was cooled to 40°C and sodium chloride (0.32 mg, 5.45 mmol) in 1 ml water was added. The reaction mixture was stirred for 1 hr. The white precipitate that formed (5-mercuro-2′-deoxyuridine) was filtered, washed with methanol and dried (*24*).

To 6 mg (8.6 μmol) of 5-mercuro-2′-deoxyuridine, 4 mg Iodogen (9.3 μmol) and sodium [^{125}I]iodide (20 mCi) in 0.3 ml water were added. The mixture was stirred at room temperature for 2 hr, filtered through a 0.22-μm Millex filter (Millipore Corp., Bedford, MA) and purified by high-performance liquid chromatography (C-18 column). The ^{125}IUdR sample was resuspended in isotonic saline and was sterilized by Millipore filtration.

Brain Tumor Model

Monolayers of exponentially growing 9L gliosarcoma cells were trypsinized, suspended in phosphate-buffered saline (PBS), pH 7.3, and kept on ice. The cells were stereotactically implanted into the right caudate nucleus of Fischer 344 rats (250–300 g). The rats were anesthetized by an intraperitoneal injection of ketamine (40 mg/kg) and xylazine (10 mg/kg) and were placed in a small-animal stereotactic frame (Kopf Instruments, Tujunga, CA). A sagittal incision through the scalp exposed the skull, and a small burr hole was made 1.3 mm posterior and 4 mm to the right of the bregma. Tumor cells (2×10^4/10 μl PBS) were injected slowly (over 30 sec) at a depth of 4 mm using a 701 Hamilton syringe. The needle was left in place for 1 min and then withdrawn slowly. The hole was plugged with bone wax and the incision was closed with surgical clips (Roboz Surgical Instrument Co., Rockville, MD).

Dosimetry

Because of the very short range (nanometer dimensions) of the electrons produced by the decay of Auger-emitting isotopes, their critical dependence on intranuclear localization for toxic effects and the heterogenous distribution of the radiopharmaceutical within the tissue of interest, classical dosimetry based on the Medical Internal Radiation Dose schema and International Commission on Radiation Units and Measurements procedures greatly underestimates the actual energy deposited in these cells (*22,25–30*). Studies were, therefore, conducted in tumor-bearing animals after intratumoral injection of the radiopharmaceutical to derive dosimetric estimates at the cellular level.

5-[^{125}I]iodo-2′-deoxyuridine (12.5 μCi) was injected stereotactically into 1-wk-old 9L tumors in the brains of Fischer 344 rats (n = 2). The brains were removed and sectioned (6 μm). The sections were fixed in methanol at −20°C, coated in NTB2 emulsion (Kodak, Rochester, NY) and stored at 4°C. After a 15-day exposure (t_{exp}), the emulsions were developed (Kodak developer D-19) for 3 min and fixed (Kodak fixer) for 5 min. The slides were then washed, stained with hematoxylin–eosin, dehydrated, and mounted in Permount (Fisher Scientific, Pittsburgh, PA). Finally, the average number of silver grains per tumor cell nucleus was determined by counting and averaging the grains present in the cell nuclei. Those nuclei with very heavy grain accumulation could not be evaluated accurately and only nuclei with 35 grains or less were counted. The total grain counts in tumor nuclei were corrected for background and the net grains per nucleus were derived. To convert the grain numbers to DNA-incorporated radioactivity (Bq/cell), a standard curve that related the grains per nucleus to emulsion exposure time was generated after the decay of a known quantity of ^{125}I in Chinese hamster V79 cells. This curve was then used to derive the exposure time (t_d) for an equivalent number of grains in 9L gliosarcoma cells (a correction was made for the size difference in the two cell lines). Finally, the intranuclear radioactive content of the 9L gliosarcoma cells (A_{9L}) was derived using the following equation:

$$A_{9L} = A_{V79} \frac{(1 - e^{\frac{-0.693 \times t_d}{T_{1/2}}})}{(1 - e^{\frac{-0.693 \times t_{exp}}{T_{1/2}}})}, \qquad \text{Eq. 1}$$

where A_{9L} and A_{V79} are, respectively, the DNA-incorporated ^{125}I activities in 9L gliosarcoma cells and V79 cells (Bq/cell), $T_{1/2}$ is the physical half-life of ^{125}I (60 days) and t_d = 54 hr. Substituting these values in Equation 1 gives $A_{9L} = 0.89 \times 10^{-3}$ becquerel/cell (0.024 pCi/cell).

To determine the cumulated activity (A_{total}) in Bq-sec/cell, the following equation was used:

$$A_{total} = A_{9L} \times \frac{T_e}{\ln 2}, \qquad \text{Eq. 2}$$

where T_e is the effective half-life of radionuclide elimination from the tumor cells.

Uptake and Diffusion of Iodine-125-IUdR in 9L Tumor and Normal Brain

To determine the relative uptake of ^{125}IUdR in 9L tumor compared with normal brain and to measure the ability of ^{125}IUdR to diffuse away from the site of injection through the interstitial fluid of the brain, 9L cells (2×10^4) were injected into the right caudate nucleus of Fischer 344 rats (Group 2, n = 5; Group 3, n = 8). Twenty-four hours later, the animals were injected stereotactically with 4 μCi ^{125}IUdR in 10 μl PBS in the tumor side (Group 2) or in the contralateral side (Group 3). In addition, 10 normal rats (Group 1) were injected stereotactically in the right caudate nucleus with 4 μCi ^{125}IUdR in 10 μl PBS. Twenty-four hours after ^{125}IUdR injection, the rats were killed and the brains were removed. The cerebellum was excised and the brain cerebrum was cut into left and right halves. The radioactivity present in each was then counted, the means ± s.e.m. were calculated and the data were analyzed using the nonparametric Wilcoxon-Gehan rank sum test.

MRI

The growth of the 9L gliosarcoma in all the rats was ascertained at various time periods by serial MRI. ^{1}H MRI was performed at 200 MHz using a Bruker Biospec 4.7 Tesla (Brukor Instruments, Billerica, MA), 30-cm imaging and spectroscopy system. A moderately T1-weighted, multislice, spin-warp imaging sequence was used (TR = 412–512 ms; TE = 25 ms) with a 5-cm field of view. The rats were anesthetized with ketamine and xylazine and then were injected with gadolinium-diethylenetriaminepentaacetic acid (DTPA) (0.5 *M*, Magnevist [Berlex Laboratories, Wayne, NJ]; 1 ml/kg intraperitoneally) to enhance relaxation in the gliosarcoma tumor. Transverse (axial) and coronal images were acquired using a 0.5-mm or 1-mm slice thickness, 256 × 256 time-domain data points and 8–12 averages.

Survival Studies

5-Iodo-2′-deoxyuridine was infused intracerebrally using Alzet osmotic pumps (Model 1007D; Alza Corp., Palo Alto, CA). In one set of experiments, ^{125}IUdR (187 μCi in 20 μl per animal; n = 11) was infused directly into 1-day-old 9L tumors over 2 days. Control animals were infused with equimolar concentrations of ^{127}IUdR (5.7 μM in 20 μl per animal; n = 11). In another set of experiments, ^{125}IUdR (238 μCi in 86 μl per animal; n = 8) was administered 9 days after tumor implantation in a 7-day infusion. Tumor-bearing control animals were infused with equimolar concentrations of ^{127}IUdR (1.33 μM in 86 μl per animal; n = 10). To prevent uptake of radioiodine by the thyroid gland, the drinking water of the tumor-bearing rats was supplemented with a 0.1% solution of potassium iodide 2 days before the start of the ^{125}I/^{127}IUdR infusion and continuing through the first 12 days.

On the day of IUdR infusion, the midline sagittal incision through the scalp that had been previously made to implant the tumor was reopened to expose the skull. The bone wax was removed from the burr hole using a 27-gauge needle. The Alzet osmotic pump was filled with 100 μl saline and connected to an L-shaped cannula (Alzet Brain Infusion Kit, Alza Corp.) by a plastic catheter that contained either nonradioactive IUdR or no-carrier-added ^{125}IUdR (specific activity 2200 Ci/mmol). Each pump was then placed in a subcutaneous pocket prepared in the midscapular area of the back of the rat using a hemostat, and the cannula was inserted through the skull to a stereotactically correct depth to allow infusion of the IUdR into the region within which the tumor had been implanted. The cannula was fixed to the skull using epoxy resin and the scalp wound was closed with surgical clips. The osmotic pump allowed IUdR to be delivered continuously to the tumor (0.5 μl/hr). The pump was removed on Day 8.

The therapeutic efficacy of intracerebrally infused ^{125}IUdR was evaluated by determining the prolongation of the median and absolute survival times of animals. Statistical analysis was performed using the Kaplan-Meier product-limit estimates followed by a Logrank test (Statgraphics, Version 6.0, Manugistics, Rockville, MD). In addition, the percent increase in life span (%ILS) was calculated.

RESULTS

Uptake and Distribution of Iodine-125-IUdR in 9L Tumor and Normal Brain

Figure 1 shows the distribution of radioactivity within the brains of the three groups of rats injected with ^{125}IUdR: Group 1, the control group, in which normal rats were injected stereotactically in the right caudate nucleus; Group 2 in which the tumor-bearing rats were injected in the right caudate nucleus (i.e., at the tumor site); and Group 3 in which the tumor-bearing rats were injected in the contralateral left caudate nucleus. Within the brains of control animals, 0.41% ± 0.05% ($\bar{x}$ ± s.e.m.) of the injected dose (ID) is retained (%ID/g = 0.24 ± 0.03) 24 hr after ^{125}IUdR injection. This indicates that the affinity of ^{125}IUdR for normal brain cells is limited and is consistent with our previous autoradiographic data where we observed the absence of DNA-incorporated radioactivity within normal brain tissue (*23*). The right hemisphere of the cerebrum (side of IUdR injection) had 69% ± 7% of the total brain uptake, the left hemisphere had 10% ± 2% and the cerebellum had 21% ± 5%. In Group 2, the percent retained in the tumor-bearing brains averaged 0.88% ± 0.20% (%ID/g = 0.46 ± 0.06). The total ^{125}IUdR brain content in these tumor-bearing animals was significantly higher ($p < 0.01$) than that in nontumor-bearing animals (Group 1). In Group 2, the right hemisphere of the cerebrum (side of tumor and of injection) had 89% ± 4% of the total brain uptake, the left hemisphere had 5% ± 2% and the cerebellum had 6% ± 3%. Compared with Group 1, the retention of ^{125}IUdR in the right hemisphere of tumor-bearing rats was significantly ($p < 0.05$) greater than that seen in the same hemisphere of nontumor-bearing rats (Fig. 1). In Group 3, the %ID retained in the brain averaged 0.39% ± 0.03% (%ID/g = 0.23 ± 0.02). The left hemisphere of the cerebrum (injection side) had 48% ± 5% of the total brain uptake, the right hemisphere (tumor side) had 16% ± 2%, and the cerebellum had 35% ± 4%. The data indicate the diffusion of ^{125}IUdR from the injection site in the left hemisphere of the cerebrum and its uptake in the tumor-bearing right hemisphere. Finally, the %ID in the right hemisphere of the rats in Group 3 (side with tumor) was significantly ($p < 0.01$) higher than that observed in the left hemisphere of nontumor-bearing animals (Group 1), demonstrating that even when the radiopharmaceutical is injected at a distance from the tumor the presence of dividing cells within the brain leads to a significant increase in radioactivity.

MRI of Intracerebral Tumors

Tumor growth was assessed by determining the location and size of intracerebral 9L gliosarcomas with serial MRI scans. Initial attempts to acquire images using a wide range of timing parameters failed to yield usable contrast between tumor and normal brain tissue. However, tumor ^1H_2O spin-lattice relaxation times can be reduced selectively by paramagnetic contrast agents introduced through the compromised blood-brain barrier (*31*). Intraperitoneal injection of gadolinium-DTPA was found

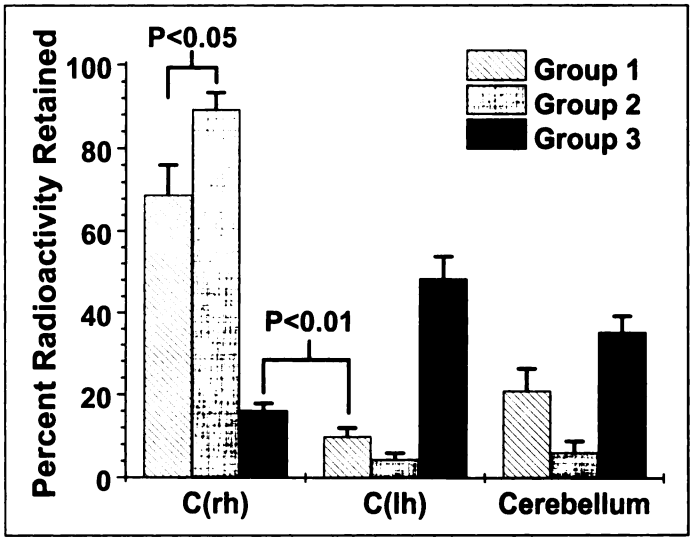

FIGURE 1. Diffusion and uptake of ^{125}IUdR after intracerebral injections in rats. Group 1, normal rats injected with ^{125}IUdR in right caudate nucleus (n = 10); Group 2, rats bearing 9L tumors in right caudate nucleus injected with ^{125}IUdR into tumor (n = 5); Group 3, rats bearing 9L tumors in right caudate nucleus injected with ^{125}IUdR into nontumor-bearing left hemisphere (n = 8). The values shown represent the means ± s.e.m. C(rh) = cerebrum, right hemisphere; C(lh) = cerebrum, left hemisphere.

to produce excellent contrast enhancement in T1-weighted images where tumors were hyperintense relative to surrounding brain tissue (Fig. 2). The needle track produced by the stereotactic injection was often visible in one or more slices, so MRI was also useful for verification of initial tumor placement. Images acquired with the infusion cannula in place exhibited a bright spot due to saline in the lumen surrounded by a dark ring corresponding to the plastic cannula itself (Fig. 2A). Local hyperintensity was often observed immediately outside the dark ring and may have been due to early tumor growth or to magnetic susceptibility artifacts arising from the tissue–cannula interface. The rapid increase in tumor size in untreated animals was clearly visible in serial MRI scans, typically yielding images such as that shown in Figure 2B a few days before death. Gliosarcoma volumes estimated from the images demonstrated an approximately exponential dependence on intracerebral incubation time (data not shown). Treatment with ^{125}IUdR slowed tumor development (Fig. 2C) and increased the time required for the tumor to reach a lethal volume.

Survival Studies

Preliminary studies demonstrated that ^{125}IUdR was stable at 37°C in Alzet pumps and plastic cannulas for up to 8 days. In the first therapeutic study, ^{125}IUdR (187 μCi in 20 μl) or ^{127}IUdR (5.7 μM in 20 μl) was infused directly during 34 hr into 1-day-old 9L tumors using an Alzet osmotic pump (Fig. 3). The median survival of animals treated with ^{125}IUdR (26 days) was markedly longer than that of control animals treated with ^{127}IUdR (18 days) and resulted in a 50% increase in the life span of the treated animals. Under this regimen, approximately 20% of the animals treated with ^{125}IUdR survived over 85 days, indicating that they may have been cured of their tumors, whereas none of the ^{127}IUdR-treated animals survived longer than 21 days.

In a second study, the therapeutic efficacy of ^{125}IUdR on 9-day-old intracerebral tumors was determined. In essence, the tumor-bearing animals were infused (100 μl/week) with either ^{125}IUdR (238 μCi in 86 μl) or ^{127}IUdR (1.33 μM in 86 μl) for 6 days directly into the tumor using an Alzet osmotic pump. For these larger and more established tumors, the median survival of animals treated with ^{125}IUdR (28.5 days) was slightly longer than that of control animals treated with ^{127}IUdR (24 days; Fig. 4) and led to a modest increase in the life span (%ILS = 22). Nevertheless, approximately 10% of the ^{125}IUdR-treated animals survived longer than 65 days and were considered cured of their tumors, whereas none of the animals in the ^{127}IUdR control group survived longer than 27 days.

In the therapy trials, the median survival of rats injected with 2×10^4 9L cells varied from experiment to experiment (17–24 days). Because the 9L cells were from the same generation, that is, the cells were frozen at the same time and one or two vials were defrosted, grown in culture and used in each of the therapy experiments, the reasons underlying this variability were not clear.

Dosimetry

The dose to radiolabeled 9L cells was determined after the intratumoral injection of 12.5 μCi of ^{125}IUdR. Because ^{125}I has a relatively long physical half-life and ^{125}IUdR is indefinitely retained after DNA incorporation, the effective half-life of radionuclide elimination (T_e) was assumed to equal the in vivo 9L doubling time of 19.3 hr (*32*). Substituting the aforementioned values in Equation 2 gives A_{total} = 89 Bq-sec/cell (89 decays/^{125}I-labeled cell/12.5 μCi injected).

DISCUSSION

5-Iodo-2′-deoxyuridine (IUdR) is a thymidine (TdR) analog in which the 5-methyl group of TdR is replaced by iodine. Since the 5-methyl group and the iodine atom have similar van der Waals' radii, this substitution gives a compound that behaves remarkably like TdR (*20,33,34*). Within the cell, IUdR is phosphorylated in a stepwise reaction (*35*) and is incorporated into the DNA of dividing cells where it is retained for the life of the cell or its progeny. Unincorporated IUdR, on the other hand, is unstable in vivo and is rapidly catabolized to iodouracil and/or is dehalogenated (*36,37*). In man, the overall half-life of IUdR in blood is less than 5 min (*38*), whereas in mice it is less than 7 min (*39*). Because the major radioactive catabolic products ($^{125}I^-$ and ^{125}I-uracil) cannot be incorporated into nuclear DNA, they will have minimal side effects on normal dividing cells. Although this in vivo instability might appear to be a negative feature for any radiotherapeutic or radiodiagnostic agent, it may prove to be an ideal characteristic for site-directed administration. When radiolabeled with an Auger-electron-emitting radionuclide (e.g., ^{125}I or ^{123}I), the therapeutic potential of ^{125}IUdR and ^{123}IUdR has already been established in mice bearing an intraperitoneal ovarian cancer (*17,40*) and in rats with leptomeningeal metastases (*18*).

Malignant gliomas are another group of tumors that may be amenable to treatment with locoregional (i.e., intratumoral) infusion of ^{125}IUdR. Because most cells within the brain are nondividing, they do not incorporate ^{125}IUdR into their DNA, allowing the agent to be taken up selectively by dividing tumor cells. Unincorporated ^{125}IUdR escapes from the central nervous system, is rapidly catabolized and becomes unavailable for incorporation into distal dividing normal cells. The potential usefulness of ^{125}IUdR for the treatment of brain tumors was supported by our earlier studies using external gamma imaging and autoradiography, which demonstrated that direct intratumoral administration of ^{123}IUdR/^{125}IUdR into intracerebral 9L gliosarcomas resulted in selective uptake of the radionuclide into tumor cells (*23*). More recently, we also examined the biodistribution of this radiopharmaceutical in patients with malignant gliomas after intratumoral administration (*41*) (and additional unpublished observations) and determined that its

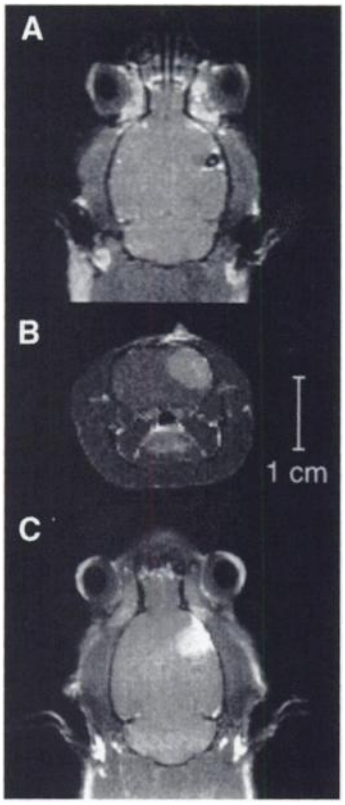

FIGURE 2. Contrast-enhanced ^{1}H MR images of rat brains after implantation of 9L gliosarcoma cells. All images are shown using same field of view. Tumors appear hyperintense relative to surrounding brain tissue. (A) Coronal image of rat during treatment. Cannula used for treatment is visible as dark ring in right caudate nucleus of brain. (B) Axial image of untreated rat acquired 16 days after implantation of tumor cells. Animal received only nonradioactive ^{127}IUdR in saline. Tumor diameter was 5–6 mm. (C) Coronal image of treated rat acquired 31 days after implantation of tumor cells. Animal received radioactive ^{125}IUdR in saline. Tumor diameter was approximately 4.5 mm.

pharmacokinetics closely resemble those seen in the rat glioma model (*23*). As a consequence of these encouraging results, we have been examining the therapeutic efficacy of intratumoral infusion of ^{125}IUdR in the intracerebral 9L gliosarcoma rat model. Because this molecule has been reported to dehalogenate rapidly, we supplemented the drinking water of the

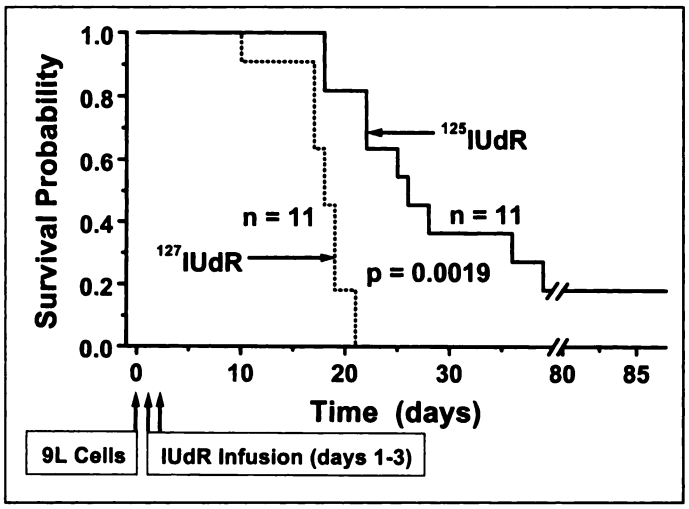

FIGURE 3. Survival of 9L-gliosarcoma-bearing rats after treatment with ^{125}IUdR. One day after tumor implantation, using Alzet osmotic pumps, tumors were infused for 34 hr with either ^{125}IUdR (187 μCi in 20 μl) or ^{127}IUdR (5.7 μM in 20 μl). When the Logrank Test is used, survival of ^{125}IUdR-treated animals is significantly (p = 0.0019) longer than that of ^{127}IUdR-infused rats.

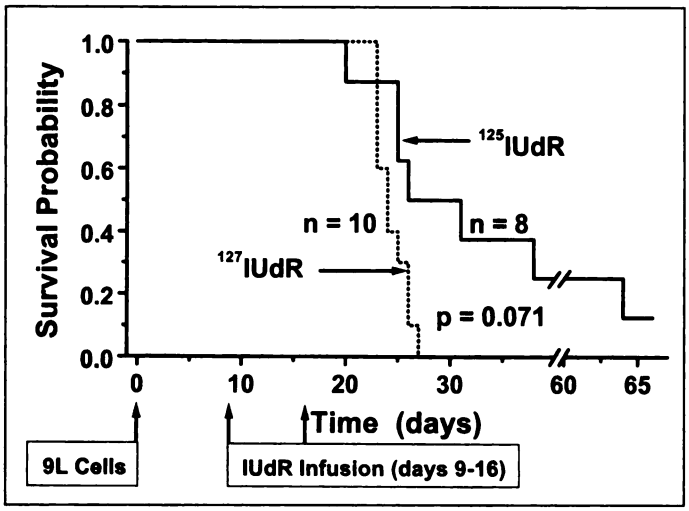

FIGURE 4. Survival of 9L-gliosarcoma-bearing rats after treatment with ^{125}IUdR. Nine days after tumor implantation, using Alzet osmotic pumps, tumors were infused for 6 days with either ^{125}IUdR (238 μCi in 86 μl) or ^{127}IUdR (1.33 μM in 86 μl). When Logrank test is used, survival of ^{125}IUdR-treated animals is significantly (p = 0.071) longer than that of ^{127}IUdR-infused rats.

tumor-bearing rats with a 0.1% solution of potassium iodide (KI) 2 days before the start of the ^{125}IUdR infusion and continuing for 12 days to prevent uptake of radioiodine into the thyroid gland, an approach that is routinely used for this purpose. In a separate series of experiments, we attempted to block the uptake of radioiodine by dissolving KI into the solution containing the therapeutic ^{125}IUdR doses and by continuously infusing the mixture into the brain through Alzet pumps. Although this approach was clearly more effective at blocking radioiodine uptake by the thyroid gland (unpublished results), it also led to the dehalogenation of ^{125}IUdR. Consequently, blockade of the thyroid was only attempted by the addition of KI to the drinking water of these animals.

An important factor that limits the effectiveness of current therapies for malignant gliomas is the tendency of the tumor cells to infiltrate into the surrounding brain tissue away from the main tumor mass. Most treatment strategies under consideration, such as brachytherapy, radiosurgery and gene therapy, are effective against the tumor mass but are limited by their inability to treat tumor cells somewhat distant from the primary site. One potential advantage of ^{125}IUdR is its small size, allowing it to diffuse in the interstitial fluid away from the primary site of injection, thus increasing the possibility of its reaching distant tumor cells. In this study, we assessed the diffusion of radiolabeled IUdR within the brain tissue and its uptake by dividing tumor cells located intracranially. The results indicate the appearance of radioactivity in the hemisphere opposite the one where the radiopharmaceutical was injected (Fig. 1), as well as in the cerebellum, thus demonstrating the ability of IUdR to diffuse to a location several millimeters from the injection site. Additionally, the injection of ^{125}IUdR into the tumor-bearing right hemisphere (Group 2) results in greater retention of activity in that hemisphere (Fig. 1), reflecting ^{125}IUdR uptake by tumor cells. The presence of increased radioactivity in the tumor-bearing hemisphere when ^{125}IUdR is injected into the contralateral side (Group 3) ascertains the presence of ^{125}IUdR (and not a catabolic/metabolic by-product) within the tissues after diffusion.

Our therapeutic studies clearly show that the locoregional infusion of ^{125}IUdR into intracranial 9L gliosarcoma solid tumors in rats significantly increases the probability of survival

and results in 10%–20% of the animals being cured of their tumors (Figs. 3 and 4). As expected, the therapeutic response was better when younger tumors were treated (1-day-old as opposed to 9-day-old). However, it is important to note that even though the two animal groups received approximately the same dose (187 μCi versus 238 μCi), it is unrealistic to directly compare the two groups because the cells were in effect exposed to varying extracellular concentrations (9 μCi/ml versus 3 μCi/ml), and the length of time that the 9L cells were bathed in ^{125}IUdR also differed (1.4 versus 6 days). Nevertheless, considering that the ^{125}IUdR doses (200 μCi) administered to the tumor-bearing rats (300 g) in our experiments are equivalent to only 50 mCi/70 kg patient, the radiopharmaceutical clears rapidly from the body (*23*), Auger-electron-emitting ^{125}I requires intranuclear localization to be effective in the mammalian cell because of its decay mode and the antineoplastic activity of ^{125}IUdR after locoregional administration in mice bearing ovarian tumor cells intraperitoneally and in rats with neoplastic meningitis does not produce overt signs of normal tissue toxicity (*17,18*), it is clear that it should be possible to administer therapeutically effective doses before the onset of detrimental side effects.

In addition to using survival as an endpoint, we examined the ability of serial MRI scans to determine the location and size of intracerebral tumors as a reflection of therapeutic efficacy. These scans showed the expected increase in intracerebral tumor volumes with time and typically yielded images such as that shown in Figure 2B a few days before the death of the animal. In untreated rats, the tumor volume estimated from the images demonstrated an approximately exponential dependence on the age of the tumor and correlated well with animal survival (data not shown). However, even though the MRI scans clearly indicated slowed tumor growth in the ^{125}IUdR-treated animals, they were not predictive of animal paralysis and death. These results are in agreement with those recently reported by Wilkins et al. (*42*) in which no significant changes in intracranial 9L tumor size was detectable in treated (radiation and/or cisplatin) animals, despite substantial tumor necrosis evident on histologic analysis.

Using the methods of Kassis et al. (*16,20*), the cumulative dose to the 9L tumor cell nucleus from the decay of DNA-incorporated ^{125}I was estimated to be 1.3 Gy/MBq of ^{125}IUdR injected (4.8 rad/μCi). In the therapy experiments reported in this article, the animals were administered 200 μCi of ^{125}IUdR and, as such, tumor cells that incorporated ^{125}IUdR received, on average, 1000 rad to their nuclei. However, recalling that the relative biological effectiveness (RBE) for DNA-incorporated ^{125}IUdR relative to x-rays (as shown by in vitro experiments) is 7.3 (*22,43*), the dose to these labeled cells in effect equals 7000 rad. Why such high doses did not lead to more effective therapeutic responses than the ones observed in our studies is probably due to the very short range (nm) of the electrons produced during the decay of Auger-electron-emitting radionuclides, the localized deposition of energy from the decaying ^{125}I atoms (*16,20,43*) and the heterogeneity of ^{125}I incorporation observed in the 9L cells, that is, many 9L tumor cells did not incorporate ^{125}IUdR. When the same calculations are performed for the commonly used beta-emitting ^{131}I isotope (maximum beta energy = 610 keV; maximum range = 2.4 mm), the dose to the nucleus from the decay of ^{131}IUdR in DNA, assuming that all the biologic factors are the same, would be only 0.087 Gy (no enhanced RBE is expected for this radionuclide) (*22,43,44*). This is not surprising since most of the energy emitted by the decay of this moderately high-energy, beta-emitting isotope will be deposited outside the cell nucleus as opposed to the decay of ^{125}I (low-energy electron emitter, high-LET-like toxicity) where the energy is deposited in the nucleus, thereby sparing possible radiation toxicity to normal tissues.

CONCLUSION

The data in this article substantiate the antineoplastic potential of ^{125}IUdR in the therapy of solid tumors that are accessible to direct administration. The findings also demonstrate the ability of this Auger-electron-emitting radiopharmaceutical to diffuse within normal tissues, thereby suggesting that ^{125}IUdR may have an important role in the eradication of microscopic tumor foci.

ACKNOWLEDGMENTS

This work was supported by the National Institutes of Health Grant RO1 CA 15523-20, Bethesda, MD.

REFERENCES

1. Levin VA, Gutin PH, Leibel S. Neoplasms of the central nervous system. In: DeVita VT Jr, Hellman S, Rosenberg SA, eds. *Cancer: principles and practice of oncology*, 4th ed. Philadelphia: JB Lippincott; 1993:1679–1737.
2. Boring CC, Squires TS, Tong T, Montgomery S. Cancer statistics, 1994. *CA Cancer J Clin* 1994;44:7–26.
3. Leibel SA, Scott CB, Loeffler JS. Contemporary approaches to the treatment of malignant gliomas with radiation therapy. *Semin Oncol* 1994;21:198–219.
4. Berger MS. Malignant astrocytomas: surgical aspects. *Semin Oncol* 1994;21:172–185.
5. Nelson DF, Curran WJ Jr, Scott C, et al. Hyperfractionated radiation therapy and bis-chloroethyl nitrosourea in the treatment of malignant glioma—possible advantage observed at 72.0 Gy in 1.2 Gy B.I.D. fractions: report of the Radiation Therapy Oncology Group Protocol 8302. *Int J Radiat Oncol Biol Phys* 1993;25:193–207.
6. Sullivan FJ, Herscher LL, Cook JA, et al. National Cancer Institute (phase II) study of high-grade glioma treated with accelerated hyperfractionated radiation and iododeoxyuridine: results in anaplastic astrocytoma. *Int J Radiat Oncol Biol Phys* 1994;30: 583–590.
7. Phillips TL, Scott CB, Leibel SA, Rotman M, Weigensberg IJ. Results of a randomized comparison of radiotherapy and bromodeoxyuridine with radiotherapy alone for brain metastases: report of RTOG trial 89-05. *Int J Radiat Oncol Biol Phys* 1995;33:339–348.
8. Wen PY, Alexander E III, Black PM, et al. Long term results of stereotactic brachytherapy used in the initial treatment of patients with glioblastomas. *Cancer* 1994;73:3029–3036.
9. Brown T. Mismatches and mutagenic lesions in nucleic acids. *Aldrichim Acta* 1995;28:15–20.
10. Hall WA. Immunotoxin therapy. *Neurosurg Clin N Am* 1996;7:537–546.
11. Barth RF, Soloway AH, Brugger RM. Boron neutron capture therapy of brain tumors: past history, current status, and future potential. *Cancer Invest* 1996;14:534–550.
12. Yung WKA. New approaches in brain tumor therapy using gene transfer and antisense oligonucleotides. *Curr Opin Oncol* 1994;6:235–239.
13. Yung WKA. New approaches to molecular therapy of brain tumors. *Curr Opin Neurol* 1994;7:501–505.
14. Kramm CM, Sena-Esteves M, Barnett FH, et al. Gene therapy for brain tumors. *Brain Pathol* 1995;5:345–381.
15. Oldfield EH. Advantages and limitations of experimental therapy of patients with malignant brain tumors with retroviral vector containing the gene for thymidine kinase and intravenous ganciclovir [Abstract]. *J Neurooncol* 1996;28:61.
16. Kassis AI, Sastry KSR, Adelstein SJ. Kinetics of uptake, retention, and radiotoxicity of ^{125}IUdR in mammalian cells: implications of localized energy deposition by Auger processes. *Radiat Res* 1987;109:78–89.
17. Bloomer WD, Adelstein SJ. 5-^{125}I-iododeoxyuridine as prototype for radionuclide therapy with Auger emitters. *Nature* 1977;265:620–621.
18. Sahu SK, Wen PYC, Foulon CF, et al. Intrathecal 5-[^{125}I]iodo-2'-deoxyuridine in a rat model of leptomeningeal metastases. *J Nucl Med* 1997;38:386–390.
19. Warters RL, Hofer KG, Harris CR, Smith JM. Radionuclide toxicity in cultured mammalian cells: elucidation of the primary site of radiation damage. *Curr Top Radiat Res Q* 1977;12:389–407.
20. Kassis AI, Fayad F, Kinsey BM, Sastry KSR, Taube RA, Adelstein SJ. Radiotoxicity of ^{125}I in mammalian cells. *Radiat Res* 1987;111:305–318.
21. Kassis AI, Howell RW, Sastry KSR, Adelstein SJ. Positional effects of Auger decays in mammalian cells in culture. In: Baverstock KF, Charlton DE, eds. *DNA damage by Auger emitters*. London: Taylor and Francis; 1988:1–13.
22. Kassis AI, Makrigiorgos GM, Adelstein SJ. Dosimetric considerations and therapeutic potential of Auger electron emitters. In: Adelstein SJ, Kassis AI, Burt RW, eds. *Frontiers in nuclear medicine: dosimetry of administered radionuclides, proceedings of symposium, 1989*. Washington, DC: American College of Nuclear Physicians; 1990:257–274.
23. Kassis AI, Van den Abbeele AD, Wen PYC, et al. Specific uptake of the Auger electron-emitting thymidine analog 5-[^{123}I/^{125}I]iodo-2'-deoxyuridine in rat brain tumors: diagnostic and therapeutic implications in humans. *Cancer Res* 1990;50:5199–5203.
24. Baranowska-Kortylewicz J, Kinsey BM, Layne WW, Kassis AI. Radioiododemercuration: a simple synthesis of 5-[$^{123/125/127}$I]iodo-2'-deoxyuridine. *Appl Radiat Isot* 1988;39:335–341.

25. Kassis AI, Adelstein SJ, Haydock C, Sastry KSR. Radiotoxicity of ^{75}Se and ^{35}S: theory and application to a cellular model. *Radiat Res* 1980;84:407–425.
26. Kassis AI, Adelstein SJ, Haydock C, Sastry KSR. Thallium-201: an experimental and a theoretical radiobiological approach to dosimetry. *J Nucl Med* 1983;24:1164–1175.
27. Sastry KSR, Rao DV. Dosimetry of low energy electrons. In: Rao DV, Chandra R, Graham MC, eds. *Physics of nuclear medicine: recent advances*. Woodbury, NY: American Institute of Physics; 1984:169–208.
28. Makrigiorgos GM, Adelstein SJ, Kassis AI. Limitations of conventional internal dosimetry at the cellular level. *J Nucl Med* 1989;30:1856–1864.
29. Makrigiorgos GM, Ito S, Baranowska-Kortylewicz J, et al. Inhomogeneous deposition of radiopharmaceuticals at the cellular level: experimental evidence and dosimetric implications. *J Nucl Med* 1990;31:1358–1363.
30. Kassis AI. The MIRD approach: remembering the limitations [Editorial]. *J Nucl Med* 1992;33:781–782.
31. Schubeus P, Schörner W, Haustein J. Dosing of Gd-DTPA in MR imaging of intracranial tumors. *Magn Reson Med* 1991;22:249–254.
32. Deen DF, Hoshino T, Williams ME, Muraoka I, Knebel KD, Barker M. Development of a 9L rat brain tumor cell multicellular spheroid system and its response to 1,3-bis(2-chloroethyl)-1-nitrosourea and radiation. *J Natl Cancer Inst* 1980;64:1373–1382.
33. Eidinoff ML, Cheong L, Rich MA. Incorporation of unnatural pyrimidine bases into deoxyribonucleic acid of mammalian cells. *Science* 1959;129:1550–1551.
34. Morris NR, Cramer JW. DNA synthesis by mammalian cells inhibited in culture by 5-iodo-2′-deoxyuridine. *Mol Pharmacol* 1966;2:1–9.
35. Bresnick E, Thompson UB. Properties of deoxythymidine kinase partially purified from animal tumors. *J Biol Chem* 1965;240:3967–3974.
36. Commerford SL, Joel DD. Iododeoxyuridine administered to mice is de-iodinated and incorporated into DNA primarily as thymidylate. *Biochem Biophys Res Commun* 1979;86:112–118.
37. Garrett C, Wataya Y, Santi DV. Thymidylate synthetase. Catalysis of dehalogenation of 5-bromo- and 5-iodo-2′-deoxyuridylate. *Biochemistry* 1979;18:2798–2804.
38. Klecker RW Jr, Jenkins JF, Kinsella TJ, Fine RL, Strong JM, Collins JM. Clinical pharmacology of 5-iodo-2′-deoxyuridine and 5-iodouracil and endogenous pyrimidine modulation. *Clin Pharmacol Ther* 1985;38:45–51.
39. Hampton EG, Eidinoff ML. Administration of 5-iododeoxyuridine-I^{131} in the mouse and rat. *Cancer Res* 1961;21:345–352.
40. Baranowska-Kortylewicz J, Makrigiorgos GM, Van den Abbeele AD, Berman RM, Adelstein SJ, Kassis AI. 5-[^{123}I]iodo-2′-deoxyuridine in the radiotherapy of an early ascites tumor model. *Int J Radiat Oncol Biol Phys* 1991;21:1541–1551.
41. Kassis AI, Tumeh SS, Wen PYC, et al. Intratumoral administration of 5-[^{123}I]iodo-2′-deoxyuridine in a patient with a brain tumor. *J Nucl Med* 1996;37(suppl 4):19S–22S.
42. Wilkins DE, Raaphorst GP, Saunders JK, Sutherland GR, Smith ICP. Correlation between Gd-enhanced MR imaging and histopathology in treated and untreated 9L rat brain tumors. *Magn Reson Imaging* 1995;13:89–96.
43. Kassis AI. Dosimetric aspects of administered radionuclides. In: Carpi A, Sagripanti A, Mittermayer Ch, eds. *Progress in clinical oncology*. Munich: Sympomed Medical Publishers; 1992:112–124.
44. Chan PC, Lisco E, Lisco H, Adelstein SJ. The radiotoxicity of iodine-125 in mammalian cells. II. A comparative study on cell survival and cytogenetic responses to ^{125}IUdR, ^{131}IUdR, and ^{3}HTdR. *Radiat Res* 1976;67:332–343.

(continued from page 7A)

FIRST IMPRESSIONS
Accumulation of Technetium-99m-MDP on the Glans Penis Secondary to Phimosis

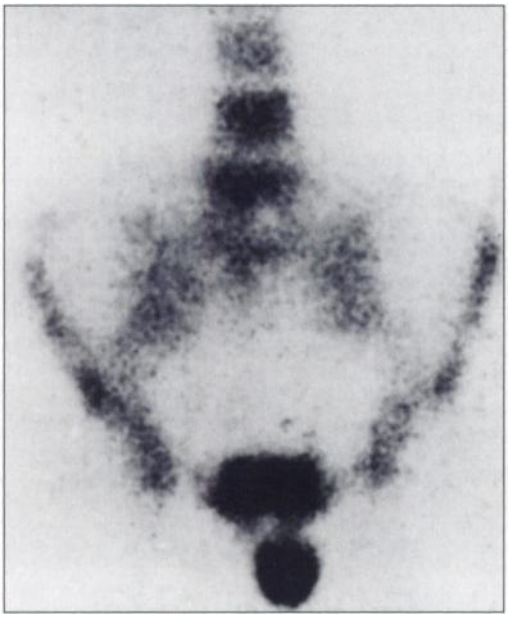

Figure 1.

PURPOSE
A ^{99m}Tc-methylene diphosphonate (MDP) whole-body bone scan was performed on a 48-yr-old man who presented with a bronchogenic carcinoma in the right upper lung field. There was no evidence of bony metastases. Accumulation of tracer was noted on the glans penis (Fig. 1). Physical examination showed redundant foreskin of the penis with a pin-point opening. Radioactive urine was retained in the space between the glans penis and the phimotic foreskin.

TRACER
Technetium-99m-MDP (700 MBq)

ROUTE OF ADMINISTRATION
Intravenous

TIME AFTER INJECTION
3 hr

INSTRUMENTATION
Elscint APEX-409 gamma camera

CONTRIBUTORS
Ren-Shyan Liu and Lee-Shing Chu, Department of Nuclear Medicine, Taipei Veterans General Hospital and National Yang-Ming University Medical School, Taipei, Taiwan